7 | The influence of pH on the reduction of CO and CO_2 to hydrocarbons on copper electrodes

Abstract

The pH is an important parameter in the reaction mechanism of the electrochemical reduction of carbon dioxide and carbon monoxide to methane and ethylene on copper electrodes. We have investigated the influence of the pH on this reaction using Cu(111) and Cu(100) single crystal electrodes. The results support our recently proposed reaction mechanism, in which two different reaction pathways to ethylene can be distinguished: a first, pH-dependent pathway that has a common intermediate with the formation of methane that occurs mainly on Cu(111), and a second, pH-independent pathway *via* a carbon monoxide dimer. The latter pathway occurs on Cu(100) only.

7.1 Introduction

The still increasing global CO_2 emissions are causing widespread concerns about the possible consequences. Mimicking photosynthesis, by reducing carbon dioxide to hydrocarbons, could be an important step forward in the reduction of carbon dioxide emissions. In this respect, an important discovery was done by Hori in the 1980s, who showed that CO_2 can be electrochemically reduced to hydrocarbons on copper electrodes.[2] Only copper electrodes have been found to catalyze this reaction to a significant extent, and the main carbon products are methane and ethylene.[3] This process could be a solution to store (surplus) sustainable electrical energy as chemical energy, that could be directly used in the current fuel (*e.g.* natural gas) infrastructure.

Since its discovery, ample research has been performed to understand the molecular mechanism of this reaction,[4,5,83,84,86,161,168] and to relate the product selectivity to the electrode surface structure.[4,5,87,88,144,166,169] A better understanding of this reaction on the molecular level could lead to an improved product efficiency and selectivity.

One important parameter in this reaction is the pH. Hori has shown that the formation of methane depends on pH, whereas the formation of ethylene is independent of pH.[84] This observation has played an important role in the various proposed molecular mechanisms.[4,84,161] Therefore, we investigate in this Chapter the influence of pH on the reduction of CO and CO_2 on Cu(100) and Cu(111). We used these electrodes because we have shown in Chapter 5 that there are two different reaction pathways from CO to ethylene:[144,170] a first pathway that has a common intermediate with the formation of methane and that takes place both at Cu(111) and Cu(100) surfaces, and a second pathway in which CO is selectively reduced to C_2H_4 at relatively low overpotentials, presumably through the formation of a surface adsorbed CO dimer. The latter pathway takes place preferentially at (100) facets, and we expect this reaction pathway to be independent of pH. We have studied the pH dependence both in phosphate buffers and in electrolytes with non-specifically adsorbing anions, using online electrochemical mass spectrometry (OLEMS).[108] This technique allows us to follow the formation of products while changing the potential at the electrode. In this way, we can measure the onset potentials for the different products as a

function of pH, and investigate the pH dependence for the different products formed.

7.2 Experimental

All experiments were carried out in an electrochemical cell using a three-electrode assembly at room temperature. The cell and glassware were boiled in ultra clean water (Millipore MilliQ gradient A10 system, 18.2 MΩ · cm) before each experiment. A gold wire was used as counter electrode and a reversible hydrogen electrode (RHE) in the same electrolyte was used as reference electrode. All potentials in this paper are referred to this electrode. The potential was controlled using an Ivium A06075 potentiostat.

The single crystal copper electrodes used were bead-type electrodes (icryst) cut and polished with an accuracy down to 0.5°. Prior to each experiment the electrode was electropolished in 66% H_3PO_4 at 3 V vs. a Cu counter electrode for 10 seconds.[154] After polishing, the surface quality was verified regularly using blank voltammetry in 0.1 M NaOH.[165]

The experiments were carried out in 0.2 M phosphate buffers, 0.2 M $NaClO_4$ solutions or 0.1 M $HClO_4$, H_3PO_4 or NaOH, all prepared from high purity reagents (Sigma-Aldrich TraceSelect, Merck Suprapur) and ultra clean water. Argon (Air Products, 5.0) bubbling was used to deaerate the electrolyte, before saturation of the electrolyte with carbon monoxide (Linde, 4.7) or carbon dioxide (Linde, 4.5).

Online electrochemical mass spectrometry (OLEMS) was used to detect the gaseous products formed during the reaction.[108] The reaction products at the electrode interface were collected with a small tip positioned close (∼50 µm) to the electrode. The tip is a 0.5 mm diameter porous Teflon cylinder with an average pore size of 10-14 µm in a Kel-F holder. This tip is connected to a mass spectrometer with a PEEK capillary. The tip configurations were cleaned in a solution of 0.2 M $K_2Cr_2O_7$ in 2 M H_2SO_4 and rinsed with ultra pure water before use. A SEM voltage of 2400 V was used, except for hydrogen ($m/z = 2$) where a SEM voltage of 1200 V was used. The products were measured while changing the potential of the electrode from 0.0 V to -1.0 V or -1.5 V with 1 mV s^{-1}. Because the equilibration of the pressure in the system after introduction of the tip in the electrolyte takes a very long time, all mass fragments show a small decay during the measurement. We corrected for this background by fitting a double exponential

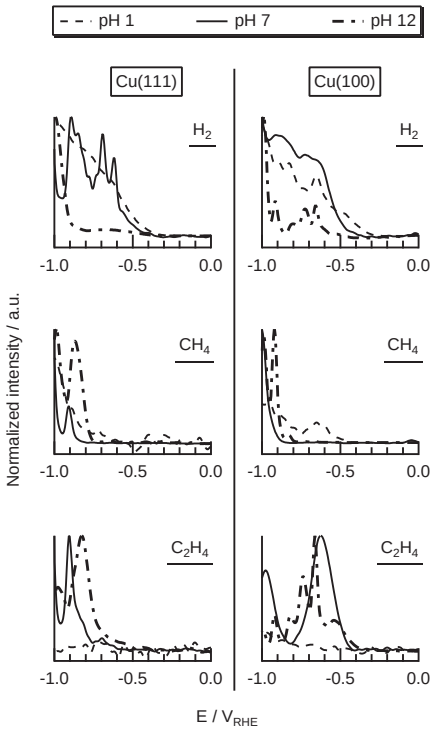

Figure 7.1 The reduction of CO in 0.1 M phosphoric acid (pH 1) and 0.2 M phosphate buffers (pH 7 and 12) on Cu(111) (left) and Cu(100) (right). With OLEMS, the formation of H_2 (m/z=2, top), CH_4 (m/z=15, middle), and C_2H_4 (m/z=26, bottom) were followed.

function to the data in the potential regions were no change in activity is observed and subtracted this fit from the data. All mass fragments shown in this paper have been background corrected in this way. In order to compare and present the various mass fragments in one graph, all mass fragments have been normalized, which is done by dividing each signal by its highest value.

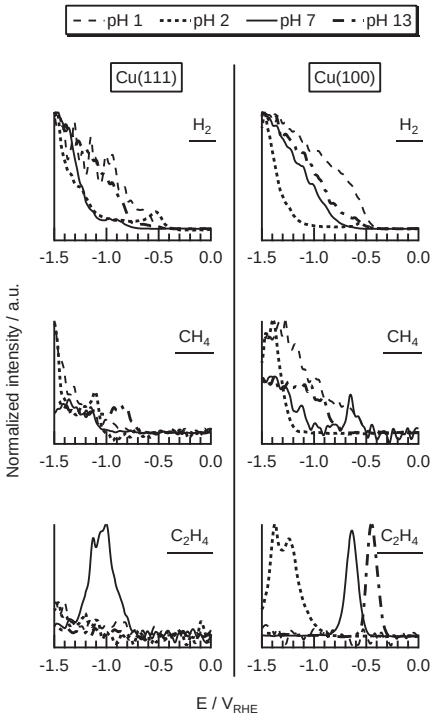

Figure 7.2 The reduction of CO in 0.1 M $HClO_4$ (pH 1), 0.2 M $NaClO_4$ (pH 2 and 7) and 0.1 M NaOH (pH 13) on Cu(111) (left) and Cu(100) (right). With OLEMS, the formation of H_2 (m/z=2, top), CH_4 (m/z=15, middle), and C_2H_4 (m/z=26, bottom) were followed.

7.3 Results

Fig. 7.1 shows the gaseous products of CO reduction in 0.1 M phosphoric acid (pH 1) and 0.2 M phosphate buffers (pH 7 and 12) on Cu(111) and Cu(100), measured with OLEMS. The three detected products are hydrogen (m/z = 2), methane (represented by m/z = 15) and ethylene (represented by m/z = 26). By comparing these three different products, it is clear that they have a different potential dependence. Both on Cu(111) and Cu(100), hydrogen formation always starts around -0.35 V, increasing with more neg-

Table 7.1 Onset potentials (on the RHE scale) for the reduction of CO

		$NaClO_4$		Phosphate buffers	
pH	Product	Cu(111)	Cu(100)	Cu(111)	Cu(100)
1	CH_4	-0.90	-0.50	-0.70	-0.45
	C_2H_4	n/a	n/a	n/a	n/a
2	CH_4	-1.0	-1.0		
	C_2H_4	n/a	-0.8		
7	CH_4	-1.1	-0.90	-0.85	-0.90
	C_2H_4	-0.75	-0.5	-0.65	-0.45
13/12	CH_4	-0.65	-0.75	-0.75	-0.75
	C_2H_4	n/a	-0.30	-0.55	-0.40

ative potentials. Interestingly, at pH 12, the hydrogen formation is limited till -0.9 V, after which it rapidly increases. The formation of methane shows some differences between Cu(111) and Cu(100) at the various pH values. At pH 1, the formation of methane is earlier on Cu(100), starting at -0.45 V. At pH 7, the formation of methane is similar on Cu(111) and Cu(100), starting at around -0.85 V. At pH 12, the formation of methane is quite similar on Cu(111) and Cu(100), starting a little earlier on Cu(111). The biggest differences are observed for the ethylene formation. At pH 1, there is only a very small fraction of ethylene observed on Cu(100). At pH 7 and 12, the formation of ethylene is much earlier on Cu(100) compared to Cu(111), and starts at around -0.4 V.

Similar experiments were performed in electrolytes with non-specifically adsorbing anions, the results of which are shown in Fig. 7.2. We have used 0.1 M $HClO_4$ (pH 1), 0.01 M $HClO_4$ + 0.19 M $NaClO_4$ (pH 2), 0.2 M $NaClO_4$ (pH 7) and 0.1 M NaOH (pH 13). Since at some pH values products were only observed below -1.0 V, we have scanned the potential till -1.5 V. The onset of the hydrogen formation in these electrolytes is similar compared the the phosphate-based electrolytes. Again, the formation of methane is earlier on Cu(100) at pH 1. Also, ethylene is not observed at pH 1. Ethylene is mainly observed on Cu(100), and the onset potential clearly shifts with pH, from -0.80 V at pH 2 to -0.30 V at pH 13. Overall, the observed potential dependence is similar in Figs. 7.1 and 7.2.

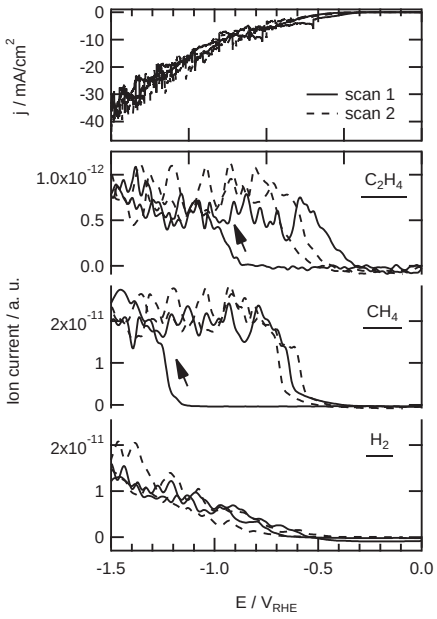

Figure 7.3 The reduction of CO in a 0.2 M phosphate buffer with pH 2 on Cu(111). The top panel shows the current density, the bottom panel the associated mass fragments for the formation of H_2 (*m/z*=2), CH_4 (*m/z*=15), and C_2H_4 (*m/z*=26) measured with OLEMS.

The onset potentials for the measurements shown in Figs. 7.1 and 7.2 are summarized in Table 7.1. From this table it can be seen again that the formation of methane starts, independent of pH, on average around -0.9 V, with Cu(100) at pH 1 as a notable exception. The formation of ethylene on Cu(100) clearly depends on pH, and shifts to less negative potentials with increasing pH.

In Table 7.1, no values are given for the measurement in a phosphate buffer at pH 2. The reason for that is shown in Fig. 7.3. In the first reduction cycle, the onset potential both for methane and ethylene is at -1.15 V. In the reverse scan, the hydrocarbon formation continues till 0.6 V(methane) or -0.4 V (ethylene). In the second scan, the onset potential for both methane

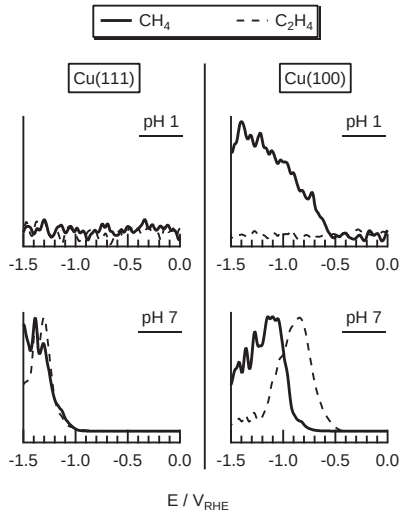

Figure 7.4 The reduction of CO_2 in 0.2 M phosphate buffers with pH 1 and 7 on Cu(111) (left) and Cu(100) (right). With OLEMS, the formation of CH_4 (*m/z*=15, green), and C_2H_4 (*m/z*=26, blue) were followed.

Table 7.2 Onset potentials (on the RHE scale) for the reduction of CO_2 in phosphate

pH	Product	Cu(111)	Cu(100)
1	CH_4	n/a	-0.55
	C_2H_4	n/a	n/a
7	CH_4	-0.95	-0.70
	C_2H_4	-0.95	-0.40

and ethylene is around -0.5 V. Fig. 7.3 shows the results for Cu(111) only, but the same phenomena was observed on Cu(100) (data not shown). This strong shift in onset potential was only observed for a phosphate buffer of pH 2.

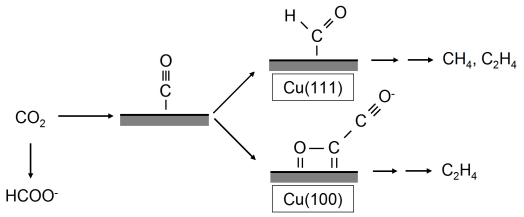

Figure 7.5 Proposed reaction mechanism for the reduction of CO_2 on Cu single crystal electrodes.[144,166]

Next to the reduction of CO, we have also investigated the reduction of CO_2. We have only studied the pH dependence of CO_2 reduction in phosphate buffers, since CO_2 itself strongly influences the pH of the unbuffered electrolytes. We could not use the phosphate buffer of pH 12, since CO_2 is completely converted to CO_3^{2-} at that pH. Therefore, we have only measured the reduction of CO_2 at pH 1 and 7, the results of which are shown in Fig. 7.4 and summarized in Table 7.2. At pH 1, methane formation starts already at -0.55 V on Cu(100), similar to the reduction of CO at pH 1 on Cu(100). On Cu(111), no reduction products of CO_2 were observed at pH 1. At pH 7, on Cu(100) ethylene formation is at lower potentials than methane formation, whereas on Cu(111) methane and ethylene have a similar potential dependence.

7.4 Discussion

7.4.1 Comparison with proposed reaction mechanism

In this section we will discuss our results for CO and CO_2 reduction at various pH values in relation to our proposed reaction mechanism presented in Chapters 3 and 5 and Ref. 166, and depicted schematically in Fig. 7.5. In Chapter 3 we have introduced a new mechanism for the electrochemical reduction of carbon dioxide and carbon monoxide on copper electrodes. We have shown that it is very likely that CHO_{ads} is the key intermediate towards the breaking of the C-O bond and, therefore, the formation of methane. This is in agreement with the observation of Hori *et al.* that the formation of methane, starting from carbon monoxide, depends on pH on the NHE scale

(independent of pH on the RHE scale).[84] For the formation of ethylene we suggested that the first step, starting from carbon monoxide, is the formation of a CO dimer, followed by the formation of an enediol(ate), or the formation of an oxametallacycle. The formation of the (negatively charged) CO dimer explains the pH-independence of reduction of CO to ethylene, as observed by Hori *et al.*[84] In Chapter 5 we have described the reduction of CO on Cu(111) and Cu(100), and we have shown that there are two different reaction pathways from CO to ethylene: a first pathway that has a common intermediate (CHO) with the formation of methane and that takes place both at Cu(111) and Cu(100) surfaces, and a second pathway in which CO is selectively reduced to C_2H_4 at relatively low overpotentials, presumably through the formation of the surface adsorbed CO dimer. The latter pathway takes place preferentially at (100) facets, as shown in Chapter 6 and supported by recent DFT calculations,[166] and this reaction pathway is independent of pH on the NHE scale (and therefore dependent of pH on the RHE scale).

From Table 7.1 we conclude that, on most surfaces, the onset potential of methane both on Cu(111) and Cu(100) is around -0.8 – -0.9 V, independent of pH. The formation of ethylene on Cu(100) shifts from -0.80 V at pH 2 to -0.30 V at pH 13 (Fig. 7.2). On Cu(111) this potential shift is much weaker, and the onset potentials for ethylene are closer to the potentials where methane formation starts. Please note that all our potentials are on the RHE scale. Since the potential of the RHE shifts with pH, a constant onset potential versus RHE at different pH values indicates a pH dependence, whereas a shift in onset potentials indicates a pH independence. Therefore, from the results presented in Figs. 7.1 and 7.2 it can be concluded that the onset potential for ethylene, in particular on Cu(100), does not depend on the pH on the NHE scale, although the observed potential-shift for the formation of ethylene is smaller than the expected 59 mV per pH unit on the RHE scale. For methane the onset potential is much more constant and, therefore, its rate-determining step involves proton transfer. Both the pH-dependent methane formation, and the pH-independent ethylene formation are in agreement with the results of Hori *et al.*[84] These results are also in agreement with our proposed reaction mechanism: the observed pH independence for the formation of ethylene on Cu(100) supports the formation of the CO-dimer on this crystal facet. Also the observation that

on Cu(111) the onset potentials for the formation of ethylene are closer to the (constant) onset potentials of methane supports a pH-dependent pathway where methane and ethylene have a common intermediate (presumably CHO).[171]

Similar conclusions can be drawn from the reduction of CO_2, presented in Fig. 7.4. At pH 7 on Cu(111), methane and ethylene are formed at the same potential. On Cu(100) at pH 7, the formation of ethylene is at a lower potential compared to methane. The reduction of CO_2 to CO and further will always be accompanied with the reduction of water, causing a local increase of pH at the electrode. This opens up a reaction pathway for the formed CO to ethylene via the CO dimer. This pathway is only available on Cu(100), and therefore we only observe a difference in onset potential for methane and ethylene on Cu(100).

7.4.2 Hydrocarbon formation at pH 1

The formation of methane and ethylene at pH 1 shows some interesting differences with the measurements at higher pH values, both for the reduction of CO and CO_2. First, there is hardly any ethylene formed at this pH, also on Cu(100). This indicates that at very low pH values the protonation of CO is favored over the formation of a CO dimer, since no ethylene is observed on Cu(100). Also the further protonation of CHO to methane is favored over the formation of the C-C bond, since also on Cu(111) hardly any ethylene is observed.

Second, it is interesting that methane formation on Cu(100) at pH 1 occurs at the lowest overpotentials, both for CO and CO_2 reduction. The formation of methane at pH 1 on Cu(100) at low overpotentials is interesting because in the literature, Cu(111) has been associated with methane formation.[87,144] In both electrolytes, at pH 1 and pH 12/13, the formation of methane starts significantly earlier on Cu(111) and Cu(100) compared to the measurements at pH 2 and 7. This shift to lower overpotentials for the formation of methane both at very low and high pH is mirrored by the formation of hydrogen. This can be best seen in Fig. 7.2, where the formation of hydrogen is higher at lower overpotentials both at pH 1 and pH 13. This high hydrogen formation at low overpotentials is most pronounced on Cu(100) at pH 1, both in phosphate and perchlorate (Figs. 7.1 and 7.2), and it is also on Cu(100) that the formation of methane has the lowest overpo-

tential at pH 1. From Fig. 7.4 we see that methane formation also occurs at lower overpotentials during CO_2 reduction on Cu(100) at pH 1. On the other hand, no methane is observed on Cu(111) during CO_2 reduction at pH 1. At present, these observations are not straightforward explained by our mechanism.

We note that also on Cu(100) at pH 7 in Fig. 7.2 we observe a small peak in m/z = 15 starting at -0.5 V already. But since this peak is in exactly the same potential region as the detection of relatively huge amounts of m/z = 26, we attribute this peak in the m/z = 15 signal to a fragment of ethylene. The relative abundances of m/z = 15 and 26 in the mass spectrum of ethylene differ by a factor of 100. In Fig. 7.2 the measured ratio is even higher, m/z = 26 is around 150 times larger than m/z = 15. Therefore, we have indicated an onset potential of -0.90 V for the formation of methane on Cu(100) in Table 7.1, and not -0.50 V.

7.4.3 CO reduction in a phosphate buffer at pH 2

We have only observed the strong potential shift between the first and second reduction cycle during the reduction of CO in a phosphate buffer of pH 2, as shown in Fig. 7.3. We may consider two different possible explanations: (1) a reconstruction of the surface and (2) a change in the pH of the electrolyte. We have investigated a possible reconstruction by performing cyclic voltammetry (CV) before and after CO reduction. Although we did observe some changes in the CV after the reduction, pointing towards a more polycrystalline surface, the most interesting observation was that when we used the same electrode again after the CV, without any modification, we observed the same shift in onset potential between the first and second reduction cycle. This indicates that the potential shift is not related to a change in surface morphology. The other explanation, a shift in the pH of the electrolyte, is also unlikely. The pH of the electrolyte is at the pK_a of the $H_3PO_4/H_2PO_4^-$ couple (K_a is the acid dissociation constant), but also the buffers at pH 7 and 12 are at the pK_a of the corresponding acid and conjugate base. Therefore, this does not explain why this potential shift is only observed at pH 2. We have also performed the reduction of CO_2 in the same electrolyte (0.1 M H_3PO_3 + 0.1 M KH_2PO_4, data not shown), but did not observe the potential shift. At present we do not have an explanation for the potential shift observed during the reduction of CO in a phosphate

buffer at pH 2. Since the potential shift is not observed in 0.01 M $HClO_4$ it could be an anion effect, but clearly this requires further scrutiny.

7.4.4 Adsorbing vs. non-adsorbing anions

Since phosphate is a strongly adsorbing anion, we have also performed the reduction of CO in electrolytes with perchlorate, a non-specifically adsorbing anion. However, the trends in onset potentials are the same in Fig. 7.1 and 7.2, and we do not observe a significant difference. Hori *et al.* have compared various anions in the electrolyte used for CO_2 reduction.[5] They have shown that in the presence of phosphate, much more hydrogen and less hydrocarbons are formed compared to *i.a.* perchlorate, sulphate and bicarbonate. This was attributed to the buffering capacity of the phosphate, which cancels the local increase in pH at the electrode surface due to the generated OH^-. Although our OLEMS cannot show absolute quantities, the relative ion currents of hydrogen, methane and ethylene in Fig. 7.1 and 7.2 support the results of Hori *et al.*; we also observe more methane and in particular more ethylene in perchlorate and hydroxide electrolytes. However, the effect is smaller than expected from literature. This could be explained by the the fact that the cations are also different in both systems. We have used potassium phosphate buffers, and sodium perchlorate and hydroxide solutions. The cation has been shown to influence the selectivity and efficiency of the CO_2 reduction.[5,172] Bigger cations increase the selectivity towards CO and hydrocarbons. Therefore, in our results the anion effect is probably partly compensated by the cation effect.

7.5 Conclusions

The observed general pH-dependence of the onset potentials for methane formation confirms the results of Hori *et al.*, showing that the formation of methane is dependent on pH. The onset potentials for ethylene formation on Cu(100) do not depend on pH, which is in agreement with our proposed reaction mechanism via the formation of a pH-independent CO dimer on this crystal facet. On Cu(111), the onset potentials for the formation of ethylene are closer to the (constant) onset potentials of methane formation. This indicates a second, pH-dependent reaction pathway to ethylene with a common intermediate (CHO) towards methane and ethylene, which is also

in agreement with our previous work. At very low and high pH, we have observed that, in particular on Cu(100), the formation of methane shifts to lower overpotentials, which is mirrored by the hydrogen formation. This indicates a relation between hydrogen evolution and methane formation, which at present is not explained by our reaction mechanism. Our reaction mechanism also does not explain why methane is not observed during the reduction of CO_2 on Cu(111) at pH 1. Also at pH 1, no ethylene formation was observed, indicating that the protonation of CO is favored over the formation of the C-C bond at low pH. In a phosphate buffer of pH 2, we have observed a shift in onset potential for methane and ethylene formation between the first and second reduction cycle during the reduction of CO. This potential shift is not related to a change in pH or surface morphology.